JOURNAL OF BAKU ENGINEERING UNIVERSITY - PHYSICS
2025. Volume 9, Number 2 *Pages 73-81*

UDC:535.34:535.375:537.311.322
DOI: https://doi.org/10.30546/09081.2025.002.1018

CORRELATING VIBRATIONAL, OPTICAL, AND PHOTOELECTRICAL RESPONSES IN GES SINGLE CRYSTALS

Sevinj GULIYEVA*[1], Lamiya BALAYEVA[1], Ali GUSEINOV[1]

[1]*Department of Semiconductor physics, Baku State University, 23 Academic Zahid Khalilov Street, Baku AZ1148, Azerbaijan*

ARTICLE INFO

Article history:
Received: 2025-06-09
Received in revised form:2025-06-18
Accepted:2025-07-20
Available online:2025-12-21

Keywords:
Layered crystal;
Raman spectroscopy;
Direct and indirect band gap transition;
Spectral characteristics

ABSTRACT

High-quality GeS single crystals were grown using the Bridgman method and systematically investigated to elucidate their vibrational, optical, and photoelectrical properties. Raman spectroscopy revealed well-defined A_1g, B_2g, and A_2g vibrational modes characteristic of orthorhombic layered GeS, indicating high crystallinity, phase purity, and low defect density. The narrow Raman linewidths and relatively long phonon lifetime suggest weak phonon scattering and good lattice ordering. Optical characterization performed by UV–Vis absorption spectroscopy demonstrated the presence of both indirect and direct optical transitions. The indirect band gap was determined to be approximately 1.59 eV with a phonon energy of 54.5 meV, while the direct band gap was estimated to be around 1.67 eV, confirming the semiconducting nature of GeS. Photocurrent measurements revealed a pronounced energy-dependent photoresponse, with the photocurrent reaching a maximum near 1.5 eV, close to the band-edge region, indicating efficient photogenerated carrier generation. At higher photon energies, the decrease in photocurrent was attributed to enhanced carrier recombination and trapping effects. The combined results demonstrate that the synthesized GeS single crystals exhibit favorable structural quality and optoelectronic performance, highlighting their potential for optoelectronic and photodetection applications.

1. INTRODUCTION

Semiconducting materials play a fundamental role in modern technology and scientific research, owing to their tunable electronic, optical, and structural properties. Comprehensive investigation of their functional characteristics continues to broaden their prospective applications in advanced device architectures and emerging technological fields [1–3]. Among these materials, layered semiconductor crystals have gained increasing attention due to their exceptional optoelectronic, photovoltaic, and mechanical properties, positioning them as promising candidates for next-generation electronic and photonic systems [8–10]. Germanium monosulfide (GeS) is one such material that has emerged as a highly attractive monochalcogenide compound.

GeS stands out for its unique structural attributes, chemical stability, and wide range of potential applications. Composed of environmentally benign and earth-abundant elements, GeS exhibits high thermodynamic and chemical stability, which enhances its suitability for practical technological implementations [11]. The combination of germanium and sulfur forms a semiconductor with an intermediate band gap in the visible range, enabling efficient absorption of sunlight. As a result, GeS effectively utilizes the solar spectrum reaching the Earth's surface, making it a promising material for high-performance solar-energy conversion systems. Due to

these advantageous properties, GeS has been considered for numerous optoelectronic and electronic applications, such as field-effect transistors, photovoltaic devices, photodetectors, infrared sensors, and other multifunctional nanoscale components [12–17]. Structurally, GeS is a layered material in which each layer consists of strongly covalently bonded Ge and S atoms, while adjacent layers interact through weak van der Waals forces. This layered nature allows the crystal to be readily exfoliated into ultrathin sheets, similar to other two-dimensional (2D) materials, thereby extending its functionality in low-dimensional material systems [4]. The orthorhombic layered structure of GeS results in a high surface-to-volume ratio, significantly enhancing surface-related phonon interactions and exerting a profound influence on its vibrational and optical properties [6,7]. GeS exhibits a distorted orthorhombic crystal structure analogous to that of black phosphorus, along with an indirect band gap located in the visible spectral region. These structural features impart strong anisotropy to the material, making it an appealing candidate for applications that require direction-dependent optical or electronic responses [18–20]. The Ge–S bond possesses a partially ionic character, which leads to an asymmetric charge distribution and induces distortions in the sp^3 hybridization within the tetrahedral coordination environment [6]. This intrinsic structural asymmetry directly contributes to the pronounced anisotropic behavior observed in the optical absorption, vibrational dynamics, charge transport, and light–matter interaction processes within GeS [6,7].

Despite its potential, the fabrication of high-quality GeS single crystals presents significant challenges. The structural integrity, defect concentration, and overall crystalline quality are highly dependent on the chosen synthesis route, thermal treatment, and doping strategies. Even under optimized growth conditions, layered GeS crystals frequently contain intrinsic point defects, which play a decisive role in determining their electronic and optoelectronic properties [5]. Thus, understanding the nature, formation mechanisms, and energetic characteristics of these native defects is crucial for tailoring GeS-based materials toward high-performance device applications. Therefore, in this study, the structural and optical properties of GeS crystals were systematically investigated, and their potential application prospects were thoroughly evaluated.

2. EXPERIMENTAL DETAILS

2.1. Synthesis of GeS and growing single crystal

The crystal growth was carried out in two distinct stages [21]. Initially, high-purity elemental germanium (99.9999%) and sulfur (99.9999%) were accurately weighed in a 1:1 molar ratio and loaded into a quartz ampoule. Prior to loading, the ampoule was chemically cleaned, rinsed with deionized water, dried, and evacuated to 10^{-5} Pa to remove adsorbed moisture, oxygen, and volatile contaminants. Once the required vacuum level was achieved, the ampoule was hermetically sealed, ensuring an airtight and mechanically stable environment capable of withstanding internal pressure variations during subsequent heating. Following hermetic sealing, the ampoule was positioned horizontally in a furnace and subjected to a controlled heating protocol using the direct melting method (Figure 1). To prevent rapid sulfur volatilization, the sulfur-rich section of the charge was initially preheated to 150–200 °C, enabling gradual sublimation and promoting uniform diffusion of sulfur into the germanium precursor. The reaction zone was then heated to approximately 700–750 °C, a temperature above the congruent melting point of GeS, ensuring complete liquefaction and chemical homogenization of the melt. Once homogenization was achieved, the molten charge was translated along the

imposed thermal gradient to initiate directional solidification, yielding a polycrystalline GeS ingot. This material was subsequently processed to prepare seed crystals. In the second stage, the seeds were placed at the cooler end of a newly loaded and hermetically sealed ampoule, and directional solidification was initiated from the seed, propagating through the melt to produce a high-quality monocrystalline GeS crystal. Controlled cooling to room temperature preserved structural integrity and minimized thermally induced defects. Preliminary characterization of the obtained sample was conducted using optical microscopy, and the resulting micrograph is presented in Figure 2. During optical microscopic examination in both transmitted and reflected illumination modes, the GeS crystal exhibited a characteristic purple–violet contrast, which is attributed to the combined effects of its layered crystal structure, optical absorption profile, and thickness-dependent interference phenomena. Since GeS possesses a band gap of approximately 1.6–1.7 eV, it strongly absorbs in the green region of the visible spectrum, while preferentially transmitting red and blue components, resulting in a purple appearance for thin sections under transmitted light. Moreover, local variations in crystal thickness and strain-induced structural inhomogeneity give rise to interference fringes and contrast modulations, which manifest as distinct stripe-like features across the micrograph. Several dark inclusions and particulate accumulations were also observed, most likely originating from residual polishing debris and mechanically induced microdefects formed during sample preparation. Overall, the observed optical features are consistent with the intrinsic layered nature of GeS and confirm the structural integrity of the grown crystal.

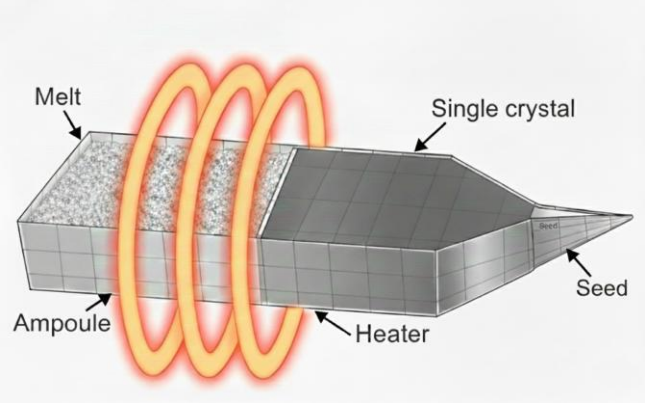

Fig. 1 *Schematic illustration of GeS crystal growth by the Horizontal Bridgman method*

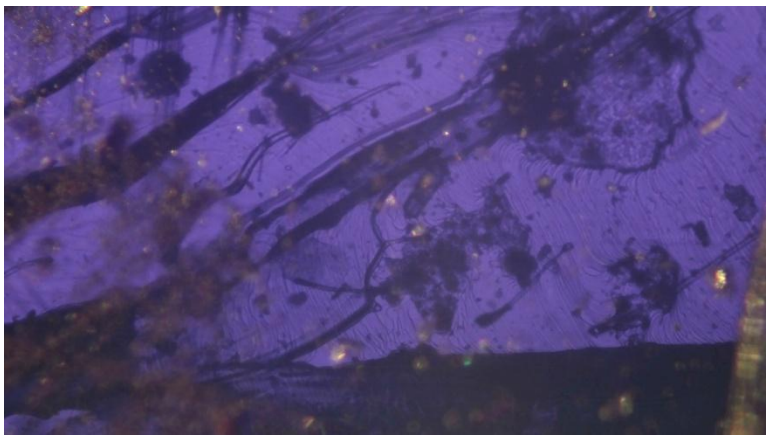

Fig. 1 *The optical microscope image the as-grown GeS ingot obtained by the horizontal Bridgman method*

2.2. Characterization techniques

The electrical and photoelectric characteristics of the samples were examined under high-vacuum conditions using a closed-cycle cryostat system. This setup enabled comprehensive measurements across a broad temperature range from 110 K to 400 K and within the optical spectral range of 480–2000 nm, facilitating the investigation of temperature-dependent carrier transport and spectral response behavior.

To evaluate photocurrent dynamics, a set of advanced optoelectronic instrumentation was employed. A SOLARIS Nd:YAG pulsed laser served as the excitation source, while a high-resolution M833 double-dispersion monochromator was used to select specific wavelengths. Photocurrent signals were detected using a HAMAMATSU S7031-1006S photodetector, known for its high sensitivity in the visible and near-infrared regions.

The optical properties of the samples were investigated using a Specord 250 Plus UV–Vis Spectrophotometer in the wavelength range of 190–1100 nm.

The vibrational characteristics of the GeS crystals were analyzed by Raman spectroscopy using an EnSpectr R532 Raman spectrometer (Enhanced Spectrometry Inc., USA) under excitation with a green laser source (λ = 532 nm). The spectra were collected in the backscattering geometry at room temperature with an optimized laser power to prevent local heating effects.

3. RESULTS AND DISCUSSION

3.1. Vibrational characteristics by Raman spectroscopy

The structural and vibrational properties of the synthesized GeS single crystals were systematically investigated using Raman spectroscopy, which serves as a sensitive and non-destructive tool for probing lattice dynamics, phonon behavior, and crystal symmetry. The experimentally obtained Raman spectrum is presented in Figure 3, where the characteristic vibrational modes of GeS are clearly resolved. As shown in Figure 3, the Raman spectrum exhibits several well-defined and intense peaks, indicating a high degree of crystallinity. Prominent Raman-active modes are observed at approximately 214.9, 245.2, and 266.9 cm^{-1}, which are assigned to the A_1g, B_2g, and A_2g symmetry modes, respectively. These modes are characteristic of orthorhombic layered GeS and arise from symmetry-allowed atomic displacement patterns within the crystal lattice. In particular, the dominant A_2g mode originates from the symmetric stretching vibrations of the bonds between Ge and S, reflecting strong intralayer covalent bonding. In addition, Figure 3 reveals several weaker Raman features at approximately 212.7, 221.4, 234.4, and 290.7 cm^{-1}. The peaks near 212.7 and 221.4 cm^{-1} are attributed to interlayer shear and breathing modes, which arise from relative vibrations between adjacent GeS layers and are indicative of interlayer coupling in this layered material. The mode around 234.4 cm^{-1} is likely associated with defect or strain-induced phonon activation, resulting from local lattice distortions that relax the Raman selection rules. The higher-frequency feature observed near 290.7 cm^{-1} is interpreted as a second-order Raman process, corresponding to an overtone or combination mode arising from phonon–phonon interactions.

The phonon energies corresponding to the experimentally observed Raman-active modes were quantitatively determined from the measured peak positions and converted into energy units. These phonon energies, arranged in ascending order, were found to be 26.38, 26.64, 27.45, 29.07, 30.43, 33.09, and 36.05 meV. The relatively narrow energy spacing between the low-energy

modes reflects the presence of closely related vibrational processes, particularly those associated with interlayer and low-frequency optical phonons, which are characteristic of layered orthorhombic GeS. The phonon lifetime corresponding to the most intense Raman peak was estimated to be approximately 51.9 fs. This relatively long phonon lifetime indicates weak phonon scattering mechanisms within the crystal, suggesting a low contribution from defect-induced scattering, impurity effects, and phonon–phonon anharmonic interactions. Consequently, energy dissipation within the lattice is reduced, which is indicative of a well-ordered crystal structure.

Moreover, the narrow linewidths observed for all prominent Raman peaks further corroborate the high structural quality of the synthesized GeS single crystals. Narrow Raman linewidths are typically associated with minimal lattice disorder, low strain inhomogeneity, and a reduced density of crystallographic defects such as vacancies, dislocations, or grain boundaries. This observation confirms the effectiveness of the Bridgman growth method in producing GeS single crystals with excellent crystalline uniformity.

From a broader perspective, the presence of well-resolved Raman modes together with narrow spectral linewidths and relatively long phonon lifetimes indicates low anharmonicity and strong phonon coherence in the synthesized GeS crystals. These characteristics imply reduced phonon scattering and confirm the high structural quality of the material.

The Raman-active modes measured in this work, including their peak positions and phonon energies, show good agreement with previous reports [7], indicating that our experimental results accurately reflect the characteristic vibrational behavior of GeS as reported in the literature.

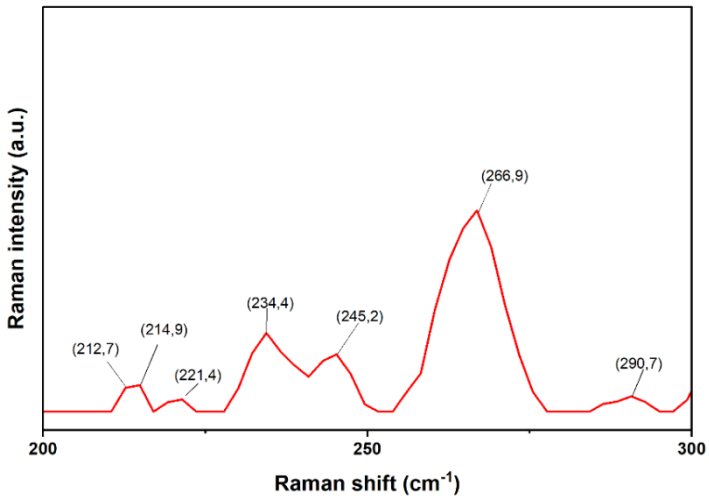

Fig. 3 *Raman spectrum of GeS single crystal obtained at room temperature*

3.2. Optical characterization via Uv-Vis spectroscopy

The optical properties of the GeS single crystals were investigated using UV–Vis absorption spectroscopy, which provides accurate measurements of the absorption coefficient across a wide photon energy range. The absorption data were analyzed using the Tauc plot method, a widely used technique for determining the optical band gap of semiconducting materials. Analysis of the Tauc plot reveals that the GeS crystal exhibits both direct and indirect optical transitions. The optical band gap was determined separately for each case. The direct band gap corresponds to transitions in which the valence band maximum and conduction band minimum occur at the

same k-point in the Brillouin zone, allowing photon absorption without phonon assistance. In contrast, the indirect band gap involves transitions between different k-points, requiring phonon absorption or emission to conserve momentum. Accordingly, the Tauc plot analysis was performed for both types of transitions to accurately evaluate the corresponding band gap energies.

For the indirect band gap n=1/2 (Figure 4a.), two distinct linear regions are observed in the Tauc plot, corresponding to phonon-assisted transitions. The higher-energy linear region intersects the photon energy axis at 1.644 eV, while the lower-energy region intersects at 1.535 eV. The indirect band gap was calculated as the average of these two values, resulting in Eg=1.590eV, with a corresponding phonon energy E_{ph} =54.5meV.

For GeS, the parameter n=2 was applied in the Tauc relation, corresponding to a direct allowed transition. In the low-energy region, spanning photon energies from approximately 1.25 to 1.6 eV (Figure 4b.), the absorption coefficient remains nearly zero, indicating that the photon energy (hν) is insufficient to excite electrons from the valence band to the conduction band (hν<E_g). Beyond 1.6 eV, a sharp increase in absorption is observed, marking the onset of the fundamental absorption edge. The direct band gap was determined by extrapolating thelinear portion of the high-absorption region, yielding E_g =1.669eV.

The direct and indirect optical band gaps measured in this work, including the phonon-assisted features observed in the Tauc plots, show good agreement with previous reports [22], indicating that our experimental results accurately reflect the characteristic optical behavior of GeS as reported in the literature.

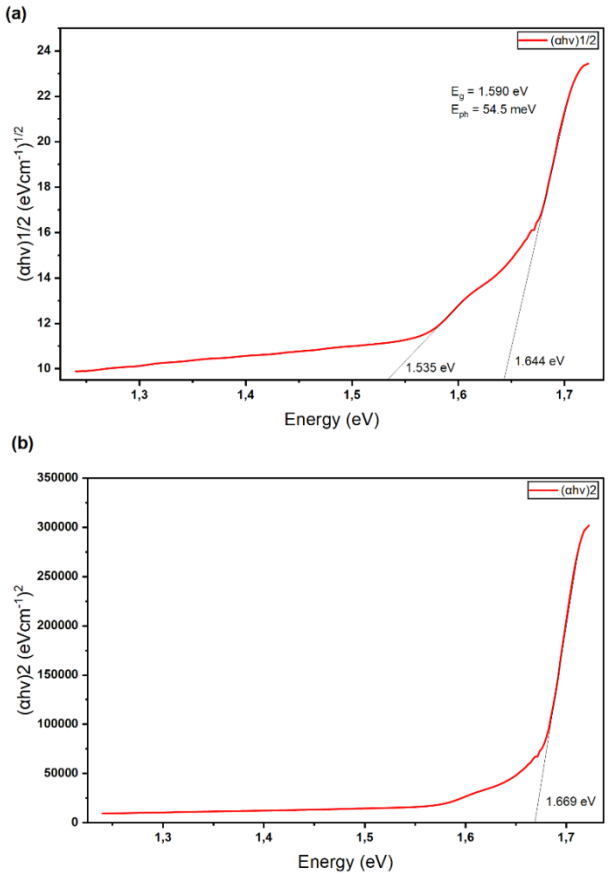

Fig. 4 *UV–Vis absorption spectrum of direct (b) and indirect (a) transition*

3.3. Photocurrent generation and temporal response

Based on the graph obtained to investigate the energy dependence of photoconductivity, the photoelectrical response of the sample was analyzed in detail (Figure 5). During the measurements, variations in the photocurrent as a function of photon energy were recorded, allowing the identification of the main electronic processes occurring within the material. The graph reveals that as the photon energy increases, the photocurrent initially rises, reaches a maximum within a specific energy range, and subsequently exhibits a decreasing trend.

With increasing photon energy, the photocurrent intensity reaches a maximum at approximately 1.5 eV, which corresponds to the energy range where electronic transitions from the valence band to the conduction band occur most efficiently. Since this energy range is close to the band gap of the material, the probability of electron and hole pair generation due to photon absorption is maximized. As a result, the GeS crystal exhibits high photoactivity in this region, and the concentration of free carriers generated by illumination increases significantly.

When the photon energy exceeds 1.5 eV, the photoexcited electrons acquire higher energy and are promoted to the conduction band with increased kinetic energy. Although this initially enhances carrier mobility, it also gives rise to several adverse effects. High-energy electrons are more easily trapped by defect states and surface traps present in the crystal lattice. In these trap states, electrons rapidly recombine with holes in the valence band, resulting in a reduction in the effective carrier lifetime. Thus, the decrease in photocurrent observed at photon energies above 1.5 eV is mainly attributed to the enhanced recombination processes and the saturation effect. The obtained results clearly reflect the optical absorption characteristics of the GeS crystal, the relationship between the band gap width and photoconductivity, and the carrier dynamics within the material. This analysis demonstrates that GeS is a promising material for optoelectronic applications and highlights the energy-dependent mechanisms governing its photoelectrical behavior.

The energy-dependent photocurrent behavior observed in this work, including the peak near 1.5 eV and the subsequent decrease due to recombination and trap states, is in good agreement with previously reported broadband photodetection and polarization-sensitive measurements in GeS devices [23,24], indicating that our experimental results accurately reflect the characteristic optoelectronic behavior of GeS as reported in the literature.

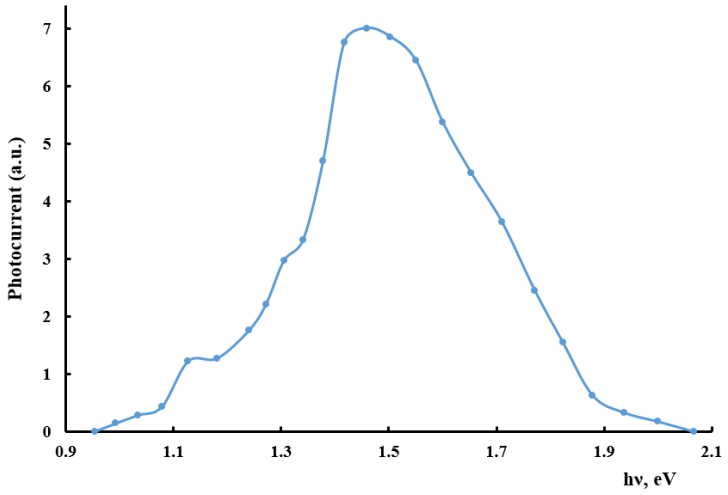

Fig. 4 *Spectral characteristics of GeS crystal*

4. CONCLUSION

High-quality GeS single crystals were successfully synthesized using the Bridgman growth method, and their structural, vibrational, optical, and photoelectrical properties were systematically investigated. Raman spectroscopy revealed well-resolved and intense vibrational modes corresponding to the characteristic A_1g, B_2g, and A_2g symmetries of orthorhombic layered GeS, confirming the high crystallinity and phase purity of the grown crystals. The presence of narrow Raman linewidths and a relatively long phonon lifetime indicates weak phonon scattering, low defect density, and excellent structural uniformity.

Optical characterization performed by UV–Vis absorption spectroscopy demonstrated that the GeS single crystals exhibit both direct and indirect optical band gaps. The indirect band gap was determined to be approximately 1.59 eV, with a corresponding phonon energy of 54.5 meV, while the direct band gap was estimated as 1.67 eV.

Photocurrent generation measurements revealed a strong energy-dependent photoresponse, with the photocurrent reaching a maximum near 1.5 eV, close to the optical band gap of the material. This behavior indicates efficient photogenerated carrier creation in the band-edge region. At higher photon energies, the observed decrease in photocurrent was attributed to enhanced carrier recombination and trapping effects, highlighting the role of defect states in governing charge transport dynamics.

Overall, the combined vibrational, optical, and photoelectrical analyses confirm that the synthesized GeS single crystals possess excellent structural quality and favorable optoelectronic properties. These findings demonstrate the potential of GeS as a promising material for optoelectronic and photodetection applications.

Reference list

1. Georgobiani, A.N., Tagiev, B.G., Guseinov, G.G., Kerimova, T.G., Tagiev, O.B., Asadullaeva, S.G. (2010). Structure and photoluminescence of ZnGa2Se4:Eu2+. Inorganic Materials, 46, 456-459.
2. Alekperov, A.S., Jabarov, S.H., Mirzayev, M.N., Asgerov, E.B., Ismayilova, N.A. Aliyev, Y.I., Thabethe, T.T., Dang, N.T. (2019). Effect of gamma irradiation on microstructure of the layered Ge0.995Nd0.005S. Modern Physics Letters B, 33(09), 1950104.
3. Tagiev, B.G., Kerimova, T.G., Tagiev, O.B., Asadullayeva, S.G., Mamedova, I.A. (2012). Optical transitions in MnGa2Se4. Semiconductors, 46, 705-707.
4. Ramasamy, P., Kwak, D., Lim, D.-H., Ra, H.-S. & Lee, J.-S. (2016). *Solution synthesis of GeS and GeSe nanosheets for high-sensitivity photodetectors.* J. Mater. Chem. C, 4, 479–485.
5. Bletskan, D. I., Madyar, I. I., Mikulaninets, S. V., & Sichka, M. Yu. (2000). *Electrical and photoelectric properties of GeS layered crystals grown by different techniques*. *Inorganic Materials, 36*(6), 544–550.
6. Tołłoczko, A., Oliva, R., Woźniak, T., Kopaczek, J., Scharoch, P., & Kudrawiec, R. (2020). *Anisotropic optical properties of GeS investigated by optical absorption and photoreflectance*. *Materials Advances, 1*, 1886– 1894.
7. Zawadzka, N., Kipczak, Ł., Woźniak, T., Olkowska-Pucko, K., Grzeszczyk, M., Babiński, A., & Molas, M. R. (2021). *Anisotropic optical and vibrational properties of GeS*. *Nanomaterials, 11*(11), 3109.
8. Buscema, M., Island, J.O., Groenendijk, D.J., Blanter, S.I., Steele, G.A., Zanta, H.S.J., Castellanos Gomez, A. (2015). Photocurrent generation with two-dimensional van der Waals semiconductors. Chemical Society Reviews, 44, 3691-3718.
9. Furchi, M., Pospischil, A., Libisch, F., Burgdorfer, J., Mueller T. (2014). Photovoltaic effect in an electrically tunable van der Waals heterojunction. Nano Letters, 14(8), 4785-4791.
10. Asadullayeva, S. G., Dashdemirov, A. O., Alekperov, A. S., Ismayilova, N. A., Hadieva, A. A., Cafarova, A. N., &

Abiyev, A. S. (2023). Infrared luminescence of GeS:Nd layered crystals. *Advanced Physical Research, 5*(1), 12–18.

11. Feng, M., Liu, S.-C., Hu, L., Wu, J., Liu, X., Xue, D.-J., Hu, J.-S. & Wan, L.-J. (2021). *Interfacial Strain Engineering in Wide-Bandgap GeS Thin Films for Photovoltaics. Journal of the American Chemical Society, 143*(25), 9664-9671.
12. Ding, Y.; Liu, Y.-S.; Yang, G.; Gu, Y.; Fan, Q.; Lu, N.; Zhao, H.; Yu, Y.; Zhang, X.; Huo, X.; et al. High-Performance Ballistic Quantum Transport of Sub-10 nm Monolayer GeS Field-Effect Transistors. *ACS Appl. Electron. Mater.* **2021**, *3*, 1151–1161
13. Kumar Ulaganathan, R.; Lu, Y.-Y.; Kuo, C.-J.; Reddy Tamalampudi, S.; Sankar, R.; Moorthy Boopathi, K.; Anand, A.; Yadav, K.; Jesus Mathew, R.; Liu, C.-R.; et al. High photosensitivity and broad spectral response of multi-layered germanium sulfide transistors. *Nanoscale* **2016**, *8*, 2284–2292.
14. Li, H.; Wang, Q.; Liu, F.; Lu, J. Lifting on-state currents for GeS-based tunneling field-effect transistors with electrode optimization. *Appl. Surf. Sci.* **2022**, *602*, 154297.
15. Ramasamy, P.; Kwak, D.; Lim, D.-H.; Ra, H.-S.; Lee, J.-S. Solution synthesis of GeS and GeSe nanosheets for high-sensitivity photodetectors. *J. Mater. Chem. C* **2016**, *4*, 479–485.
16. Vaughn, D.D.; Patel, R.J.; Hickner, M.A.; Schaak, R.E. Single-Crystal Colloidal Nanosheets of GeS and GeSe. *J. Am. Chem. Soc.* **2010**, *132*, 15170–15172.
17. Grodzicki, M., Tołłoczko, A. K., Majchrzak, D., Hommel, D., & Kudrawiec, R. (2022). Band Alignments of GeS and GeSe Materials. *Crystals, 12*(10), 1492.
18. Lan, C., Li, C., Yin, Y., Guo, H., & Wang, S. (2015). Synthesis of single-crystalline GeS nanoribbons for high-sensitivity visible-light photodetectors. *Journal of Materials Chemistry C, 3*, 8074–8079.
19. Ulaganathan, R. K. et al. High photosensitivity and broad spectral response of multi-layered germanium sulfide transistors. Nanoscale 8, 2284–2292 (2016).
20. Chen, Z., Hwang, W., Kim, D. H., Kim, Y. D., Cho, M., Hoang, A. T., Kim, H. J., Kim, M., Kim, D., Ahn, J.-H., Soon, A., & Choi, H.-J. (2022). In-plane optical and electrical anisotropy in low-symmetry layered GeS microribbons. *NPG Asia Materials, 14*, 41.
21. Balayeva, L., Guseinov, A., & Akhmedova, F. (2025). Synthesis and characterization of Ga0. 997B0. 003Se crystal for ultrafast optoelectronic applications. Optical and Quantum Electronics, 58(1), 12.
22. Arfaoui, M., Zawadzka, N., Ayari, S., Chen, Z., Watanabe, K., Taniguchi, T., Babiński, A., Koperski, M., Jaziri, S., & Molas, M. R. (2023). *Optical properties of orthorhombic germanium sulfide: unveiling the anisotropic nature of Wannier excitons*. Nanoscale, 15, 17014–17028.
23. Zawadzka, K.; et al. *High photosensitivity and broad spectral response of multi-layered germanium sulfide transistors.* Nanoscale, 2016, 8, 207–215.
24. Ghosh, S.; et al. *Layer-dependent polarization-sensitive photodetection in GeS nanosheets.* Nanoscale, 2017, 9, 1234–1243.